Journal of Bioscience and Bioengineering
VOL. 127 No. 2, 222–230, 2019

www.elsevier.com/locate/jbiosc

Structural characterization of hemicellulose released from corn cob in continuous flow type hydrothermal reactor

Tsutomu Arai,[1] Peter Biely,[2] Iveta Uhliariková,[2] Nobuaki Sato,[1,3] Satoshi Makishima,[1,3] Masahiro Mizuno,[1,4] Kouichi Nozaki,[1,4] Satoshi Kaneko,[5] and Yoshihiko Amano[1,4,*]

Department of Chemistry and Material Engineering, Faculty of Engineering, Shinshu University, 4-17-1 Wakasato, Nagano 380-8553, Japan,[1] Institute of Chemistry, Slovak Academy of Sciences, Dúbravská Cesta 9, 845 38 Bratislava, Slovak Republic,[2] B Food Science Co. Ltd., 24-12 Kitahamamachi, Chita 478-0046, Japan,[3] Institute of Engineering, Academic Assembly, Shinshu University, 4-17-1 Wakasato, Nagano 380-8553, Japan,[4] and Department of Subtropical Bioscience and Biotechnology, University of the Ryukyus, Nishiara, Okinawa 903-0213, Japan[5]

Received 26 March 2018; accepted 18 July 2018
Available online 22 August 2018

Hydrothermal reaction is known to be one of the most efficient procedures to extract hemicelluloses from lignocellulosic biomass. We investigated the molecular structure of xylooligosaccharides released from corn cob in a continuous flow type hydrothermal reactor designed in our group. The fraction precipitable from the extract with four volumes of ethanol was examined by ^{1}H-NMR spectroscopy and MALDI-TOF MS before and after enzymatic treatment with different purified enzymes. The released water-soluble hemicellulose was found to correspond to a mixture of wide degree of polymerization range of acetylarabinoglucuronoxylan fragments (further as corn cob xylan abbreviated CX). Analysis of enzymatic hydrolyzates of CX with an acetylxylan esterase, GH3 β-xylosidase, GH10 and GH11 xylanases revealed that the main chain contains unsubstituted regions mixed with regions of xylopyranosyl residues partially acetylated and occasionally substituted by 4-*O*-methyl-D-glucuronic acid and arabinofuranose esterified with ferulic or coumaric acid. Single 2- and 3-*O*-acetylation was accompanied by 2,3-di-*O*-acetylation and 3-*O*-acetylation of Xyl*p* residues substituted with MeGlcA. Most of the non-esterified arabinofuranose side residues were lost during the hydrodynamic process. Despite reduced branching, the acetylation and ferulic acid modification of pentose residues contribute to high yields and high solubility of the extracted CX. It is also shown that different enzyme treatments of CX may lead to various types of xylooligosaccharides of different biomedical potential.

[**Key words:** Xylo-oligosaccharide; Corn cob; Hydrothermal reaction; Matrix-assisted laser desorption/ionization time of flight mass spectrometry; Acetylation]

Hemicelluloses are the principal components of plant cell walls that form a complex three-dimensional structure with the other principal cell wall components, cellulose and lignin. In contrast to cellulose, hemicelluloses are usually water soluble and, as a rule, represented by heteropolymers consisting of several different monosaccharides and organic acids. Hemicelluloses show great variations in plant species, and even in different organs of the same plant (1–3). There are also varieties of the major plant hemicellulose, xylan. A common structural feature of xylans is the backbone built of β-1,4-linked xylopyranosyl (Xyl*p*) residues. In most cases, xylans contain acetic acid esterifying the main chain Xyl*p* residues at position 2 or at position 3 or at both positions (4–8). The xylan side substituents which show the greatest variety in different plant species, are α-1,2-linked D-glucuronic acid (GlcA) or 4-*O*-methyl-D-glucuronic acid (MeGlcA), and α-1,3-linked L-arabinofuranosyl (Ara*f*) residues. In xylan of annual plants, like cereals, the Ara*f* residues are frequently esterified at position 5 by phenolic acids, such as ferulic or *p*-coumaric acid (9–11). The xylan branching, prevents crystallization of the polysaccharide molecules similar to that of cellulose, regulates xylan association with cellulose and is also responsible for high hydration and solubility of xylan. At the same time, xylan side substituents protect xylopyranosyl linkages from hydrolysis by microbial enzymes (12). Thus, the branching leads not only to enhanced resistance of hemicellulose but also protects the xylan-associated cellulose against invading microorganisms. Therefore, a comprehensive elucidation of the structural features of extracted xylan, including information about the acetylation and other substitutions, is important for development and application of processes for efficient utilization of lignocellulosic biomass, including rational design of hemicellulose-based prebiotics.

To extract or remove xylans from lignocellulosic biomass, alkaline extraction methods have been widely used (10,11,13–16). However, the structure and properties of saccharide chains extracted in this way do not correspond to the native plant polymers, because alkaline treatments result in saponification of ester linkages. Esterified hemicellulose, structurally resembling that in the plant cell walls, can be obtained under non-alkaline conditions such as hot water extraction, organosolvent and partially also by steam explosion and autohydrolysis at increased pressure and temperature (6,11,17–26). The degree of xylan

* Corresponding author at: Institute of Engineering, Academic Assembly, Shinshu University, 4-17-1 Wakasato, Nagano 380-8553, Japan. Tel./fax: +81 26 269 5394.
E-mail address: yoamano@shinshu-u.ac.jp (Y. Amano).

1389-1723/$ – see front matter
https://doi.org/10.1016/j.jbiosc.2018.07.016

degradation and deacetylation depends on severity of the extraction process (27).

Corn cobs belong to the most frequently used raw material for isolation of hemicellulose xylan and xylooligosaccharides (6,14,28). We have developed a continuous flow type hydrothermal reactor (flow rate: 20 L/h) which afforded high yields of soluble xylan from milled corn cob using a short time of high temperature treatment (29). A size exclusion chromatography of the released water-soluble material showed the presence of fragments with degree of polymerization (DP) ranging from 2 to more than 20, however, we did not pay attention to esterification of the released xylan and xylooligosaccharides (29). It is also well known that different result was obtained when the equipment was scale-up. In addition, we focused on chemical nature of this material as sufficient weight of corn cob xylan (CX) fraction after hydrothermal treatment has been obtained. The ethanol precipitate of hydrothermally extracted CX was analyzed by proton nuclear magnetic resonance (^{1}H-NMR) spectroscopy, and its fragments generated with several purified enzymes and the hydrolyzates were analyzed by matrix-assisted laser desorption/ionization time of flight mass spectrometry (MALDI-TOF MS) and thin-layer chromatography (TLC). Here we show that extracted CX is depleted in Ara*f* and that a considerable portion of Xyl*p* residues in CX are acetylated and also substituted with Ara*f* residues esterified with ferulic acid (FeA) and *p*-coumaric acid (CouA). The acetyl groups can be removed by acetylxylan esterase (AcXE) with the exception of the 3-*O*-acetyl group at the MeGlcA-substituted Xyl*p*. Several lines of evidence suggested that hydrothermal extraction preserves in CX mainly the side substituents at regions more densely acetylated or substituted with Ara*f* esterified with phenolic acids. The CX can be converted by purified xylanases to linear and branched acetylated oligosaccharides of various degrees of polymerization and acetylation.

MATERIALS AND METHODS

Preparation of soluble saccharides from corn cob in the continuous flow type hydrothermal reactor Dried corn cob imported from Thailand was supplied by B Food Science Co., Ltd. (Tokyo, Japan). The corn cob was grounded to a powder from which a fraction with diameter of approximately 30–60 μm was obtained by sieving. The composition of dry corn cob was reported in our previous work ((29)): glucan (mainly cellulose), 29.7%; xylan, 29.9%; arabinan, 3.4%; Klason lignin, 12.7%; acid-soluble lignin, 2.6%; ethanol–benzene extractives, 2.7%; ash, 3.5%; others (by difference), 15.5%. The powder was suspended in tap water at a concentration of 13% (w/v) and processed in the continuous flow type hydrothermal reactor as previously described (29). The optimized hydrothermal reaction (190 °C, 13 min heating time during continuous process) released large amounts of hemicellulose into solution.

The extract was clarified by centrifugation and the hemicellulose in the supernatant was precipitated with four volumes of ethanol and left to stand overnight at 4 °C. The precipitate was recovered on a Gooch crucible type filter 2G3 (AGC Techno Glass, Shizuoka, Japan), washed twice with ethanol and twice with acetone and then vacuum-dried. About 23 g of light brown corn cob xylan (CX) was obtained from 1 L of the reactor liquid which corresponds to 18% of the weight of the starting raw material.

High performance liquid chromatography analysis Quantitative analysis of neutral sugars and hydroxycinnamic acids was done by high performance liquid chromatography (HPLC) carried out as previously described (30,31). For monosaccharide compositions, a 3% solution of CX was boiled in 1 M H_2SO_4 for 3 h and then neutralized by a saturated solution of $Ba(OH)_2$. After removing insoluble $BaSO_4$ by centrifugation and filtration, monosaccharides were determined by HPLC on an Aminex HPX-87 P column (BioRad, Hercules, CA, USA) using a refractive index detector. Amounts of acetic acid formed by acid hydrolysis of acetyl esters, was also analyzed using a RI detector. The FeA and CouA content was determined by HPLC after alkaline de-esterification in 1 M NaOH at 65 °C for 2 h and subsequent neutralization with an aqueous HCl solution. HPLC was done on an Inertsil ODS-3 column (GL Sciences, Tokyo, Japan) using an ultraviolet (UV) detector. The content of uronic acids was determined using the H_2SO_4/2-hydroxydiphenyl reagent (32).

Enzymes Two endo-β-1,4-xylanases from *Streptomyces olivaceoviridis*, which belongs to glycoside hydrolase (GH) family 10 and 11 and the *Aspergillus niger* β-xylosidase belonging to GH family 3 were prepared as described (33,34). A GH3 β-xylosidase was purified from a commercial cellulase preparation from *Penicillium funiculosum* (Sigma-Aldrich, St. Louis, MO, USA). Briefly, the enzyme powder was suspended in 50 mM phosphate buffer, pH 6.0, for 12 h. After removal of insoluble materials by centrifugation, the supernatant was applied onto Q-Sepharose FF column and eluted by a linear gradient of NaCl (0–250 mM). The fraction containing β-xylosidase activity was then applied onto CM-Sepharose FF column equilibrated in 10 mM acetate buffer, pH 4, and eluted by a linear gradient of NaCl (0–250 mM). *Orpinomyces* CE6 AcXE was from Megazyme Int. (Wicklow, Ireland). Amyloglucosidase from *Rhizopus* mold and α-amylase from *Bacillus subtilis* were from Sigma. Both amylolytic enzymes were shown to be free of xylanolytic enzymes.

Enzymatic treatment of the extracted CX by hydrothermal reaction The presence of acetyl substituents in CX and its deacetylation by *Orpinomyces* sp. CE6 AcXE were examined by ^{1}H-NMR spectroscopy at 25 °C (see below). CX was dissolved in D_2O (10 mg/0.6 ml) and pH of the solution was adjusted to pH 6.0 by addition of deuterated sodium acetate, and then the first NMR spectrum measured. After addition of the CE6 AcXE (lyophilized three times from D_2O, final concentration 0.05 mg/ml) the changes of the signals of the acetyl groups were monitored.

A solution of CX in deionized water (1%, w/v), adjusted to pH 5.5, was incubated separately with GH3 β-xylosidase and two *S. olivaceoviridis* endo-β-1,4-xylanases belonging to GH10 and GH11 (enzyme concentrations between 10 and 30 μg/mL) at 37 °C for 16 h under a toluene layer to avoid microbial contamination. The proper amount of enzymes to achieve maximum CX degradation was selected on the basis of preliminary experiments performed on 1% deacetylated birchwood xylan (Wako Pure Chemical, Osaka, Japan). Final GH10 and GH11 xylanase hydrolyzates were heated (100 °C, 5 min to denaturate the enzymes) and their aliquots subsequently incubated with β-xylosidase. The enzymatic hydrolyzates were analyzed by one and two-dimensional TLC and MALDI-TOF MS.

In some experiments the α-1,4-glucan and α-1,4-glucooligosaccharides contaminating the extracted CX were eliminated by treatment with a mixture of amyloglucosidase and α-amylase (0.2 mg or 2 mg/g of CX in 10 ml of water) at 35 °C for 4 d. After thermal denaturation of the enzymes (100 °C for 5 min) and cooling, the non-hydrolyzed polysaccharides were recovered by precipitation with three volumes of ethanol.

NMR spectroscopy NMR measurements were performed in D_2O at 25 °C on VNMRS 400 MHz Varian spectrometer equipped with 5 mm ^{1}H–^{19}F/^{15}N–^{31}P PFG AutoX DB NB probe head with an automatic chemical shifts calibration. Advanced techniques from Varian pulse sequence library of 2D homo- and hetero-correlated spectroscopy and literature data were used for the signal assignments. The detailed procedure for the NMR measurements was described previously (35).

MALDI-TOF MS analysis Solutions of CX or its enzymatic hydrolyzates (1%, w/v) were diluted 10-fold with deionized water, and treated with Amberlite IR120B HAG (H^+-form). After removing of Amberlite, the sample solutions were supplemented with 50 mmol/L NaCl. A 0.5 μL of the matrix solution of 2,5-dihydroxybenzoic acid (Tokyo Chemical Industry, Tokyo, Japan) in 30% acetonitrile (9 mg/mL) was applied on a stainless steel target plate and immediately mixed with equal volume of the sample solution. Air-dried samples were analyzed within the MALDI-TOF MS instrument AXIMA CFRplus (Shimadzu, Kyoto, Japan). Operation of the instrument, spectroscopy measurements, and analyses of the data were managed with the Kompact software (Kratos Analytica, Manchester, UK). The parameters of the MS were optimized and calibrated using xylooligosaccharide standards.

TLC analysis of oligosaccharides Enzymatic hydrolyzates of the extracted CX fraction were analyzed by TLC on silica gel 60-coated aluminum sheets (Merck, Darmstadt, Germany) in 1-butanol-ethanol-water (60:15:12, v/v) in one or two dimensions. Between the two developments, oriented by 90° one to another, the dried chromatograms were exposed to ammonium hydroxide vapors overnight to saponify all acetylated or by phenolic acid esterified oligosaccharides (36). Deesterification leads to slower migration of the compounds in the second dimension, so in contrast to non-esterified compounds they appear below the diagonal. Carbohydrates were detected using *N*-(1-naphtyl)ethylenediamine dihydrochloride reagent (37). A few more abundant oligosaccharides containing phenolic acids could be detected under UV light (366 nm) on fresh dried chromatograms.

TLC was also used to determine the portion of CX converted by xylanases to shorter oligosaccharides migrating from the starting line. In the used solvent system the migration of non-esterified oligosaccharides from the starting line is limited to about DP 8. This limit would be higher for esterified oligosaccharides. After elution of the plate and detection of guide strips, silica gel with compounds released by xylanases and the material staying on the starting line were separately eluted twice with l mL of water. The sample untreated with enzymes was used as a control. Eluates, clarified by centrifugation and filtration, were evaporated in a vacuum, dissolved in 0.2 mL and total carbohydrates were determined by phenol-sulfuring acid method (38).

RESULTS

Composition of isolated CX fraction by hydrothermal reaction The hydrothermal treatment of milled corn cob afforded a dark brown and sweet-smelling liquid containing mainly partially degraded CX which was isolated by precipitation with four volumes of ethanol as a dry light brown powder. This step led to separation of low molecular mass compounds such as monosaccharides, short oligosaccharides and part of phenolics derived from lignin causing reddish color of the supernatant.

The content of monosaccharides and organic acids in CX was determined by HPLC of its acid hydrolyzate (Table 1). As expected, xylose was the main monosaccharide component, while glucose, arabinose, mannose and galactose were present in low amounts. Acetic acid, FeA, and CouA were observed in significant amounts. Methanol was undetectable. The molar ratio of xylose to arabinose shows that every 23rd Xyl*p* residue is substituted with Ara*f* residue. This ratio was about 9 in the starting corn cob. The content of FeA and CouA indicates that two thirds of the residual Ara*f* side chains are esterified with these two phenolic acids. This means that hydrothermal processing led to depletion of non-esterified Ara*f* side residues. The molar ratio of xylose to acetic acid (Table 1) suggests that approximately every fifth to sixth xylopyranosyl (Xyl*p*) residue carries one acetyl group. The degree of substitution by uronic acids appears to be similar to that by esterified Ara*f*. As we shall see below, the uronic acid appears to be mainly MeGlcA.

Structural features deduced from NMR spectroscopy The anomeric region and the region of signals of protons of methyl acetyl groups of the ^{1}H-NMR spectrum of isolated CX is shown in Fig. 1 (bottom spectrum). The assignments of signals was based on published information (4,35) and also on basis of the HSQC spectrum (Fig. 2). The spectrum shows, beside the largest signal of internal Xyl*p* residues (Xyl, H1 at 4.45 ppm), signal of the α-anomer of the reducing end Xyl*p* residue ($Xyl_{red\alpha}$, H1 at 5.16 ppm) and signals of Xyl*p* residues acetylated at positions 2 or 3. These two types of acetylation are also documented by chemical shifts of protons of the acetyl methyl groups at 2.13 and 2.14 ppm. This region of the spectrum also contains two weaker signals; one corresponds to the 3-*O*-acetyl group on Xyl*p* residue 2-*O*-substituted with MeGlcA (at 2.20 ppm) and other to two overlapping signals of 2,3-di-*O*-acetylated Xyl*p* (at 2.08 ppm) (35). The 3-*O*-acetylation of MeGlcA-substituted Xyl*p* residues is confirmed by the HSQC spectrum (Fig. 2). The signal at 2.20 could also belong to the 2-*O*-acetyl group on Xyl*p* 3-*O*-substituted with Ara*f* residues or to such residues 5-*O*-esterified with phenolic acids (39). The anomeric region of the spectrum contains the H1 signal of α-1,4-linked Glc*p* residues (at 5.38 ppm) corresponding to co-extracted α-1,4-glucan. Fig. 3, displaying the H-signals of phenolic acids, namely of *trans*-ferulic acid (40), shows that the signal of α-1,4-glucan disappeared after treatment of CX with xylanase-free amyloglucosidase and α-amylase. Fig. 3 also confirms the presence of MeGlcA. The signal at 5.27 ppm is assigned to H1 of MeGlcA because its 4-*O*-methyl signal was also detected in the HSQC spectrum (Fig. 2). The H1 signals of 5-feruloylated Ara*f* could be hidden in the same region (5.25–5.35 ppm) (39,40). The resonance at 5.51 ppm could correspond to H-1 of the Ara*f* side residues 2-substituted with α-Gal*p* (39,41).

TABLE 1. Composition of CX isolated using the continuous flow type hydrothermal reactor.

Component	Content			Molar ratio[a] (Xyl:Y)
	(mg/g)	(mmol/g)		
Sugars				
Xylose	535	3561	(Xyl)	
Glucose	121	672		
Arabinose	23	153	(Y)	23
Mannose	19	104		
Galactose	18	98		
Uronic acids	36	176	(Y)	20
Substituents				
Acetyl group	39	645	(Y)	5.5
Feruloyl group	14	73	(Y)	49
p-Coumaroyl group	4	26	(Y)	137

[a] Molar ratio of the component to xylose (mol/mol).

Enzymatic deacetylation by CE6 AcXE Fig. 1 shows that resonances corresponding to 2-*O*-, 3-*O*-mono- and 2,3-di-*O*-acetylated Xyl*p* residues in the anomeric region and to protons of methyl groups of the acetyl groups (signals between 2.08 and 2.14 ppm) of isolated CX were reduced on incubation with AcXE. The enzyme removed efficiently the acetyl groups from singly and doubly acetylated Xyl*p* residues, but ignored the 3-*O*-acetyl group on Xyl*p* 2-*O*-substituted with MeGlcA (signal at 2.20 ppm). These results show that CX extracted in the continual hydrothermal reactor can be deacetylated enzymatically.

MALDI-TOF MS analysis of CX extracted in the continual hydrothermal reactor More information on the character of isolated CX was obtained by MALDI-TOF MS analysis. The spectrum in Fig. 4A shows sodium adduct ions ($[M+Na]^{+}$) of unsubstituted (shown as arrows in the figure) and to a different degree acetylated oligosaccharides ranging from DP 4 to 12. All short ionizable fragments correspond to compounds present in at very low concentration because the TLC examination of isolated CX showed negligible amounts of saccharides migrating from the starting line (Fig. S1). The MS spectrum did not show any ions of products containing phenolic acids esterifying Ara*f* residues, neither ions of oligosaccharides containing MeGlcA residues.

Effect of GH3 β-xylosidase, GH and GH11 xylanases Incubation of isolated CX with the GH3 β-xylosidase, resulted in disappearance of ions of all non-acetylated oligosaccharides suggesting that they are linear β-1,4-linked xylooligosaccharides (Fig. 4A, arrows). Simultaneously, ions of many new, mainly highly acetylated oligosaccharides, such as ions of Xyl_4Ac_2, Xyl_4Ac_3, Xyl_5Ac_2, Xyl_5Ac_3, Xyl_6Ac_3 and Xyl_6Ac_4, appeared in the region of compounds of lower DP (Fig. 4B). In the region of larger acetylated products, β-xylosidase treatment led to disappearance or decrease of signals of oligosaccharides with low number of acetyl groups, and appearance or increase of signals of those with a higher degree of acetylation and substitution with α-L-Ara*f* esterified with phenolic acids, such as Xyl_2AraFe, Xyl_3AraFe, $Xyl_3AcAraFe$, Xyl_4AraFe, Xyl_5AraFe, and $Xyl_5AcAraFe$ (Fig. 4B, see inclined arrows). Based on the fact that β-xylosidase hydrolyzed completely the non-acetylated oligosaccharides from non-reducing end, the survived acetates or AraFe-substituted oligosaccharides must carry at least one substituent on the non-reducing end Xyl*p* residue blocking further action of β-xylosidase.

We should also mention that careful examination of mass spectra provided evidence for ions of oligosaccharides in which FeA is replaced by CouA. However, since the molecular mass of CouA is the same as GlcA, the mentioned ions could correspond also to non-methylated aldouronic acids.

Before MS analysis of CX fragments generated by GH10 and GH11 xylanases, we evaluated the degree of CX conversion to oligosaccharides migrating on TLC from the starting line (Fig. S1). This fraction includes non-acetylated oligosaccharides approximately up to DP 8 and also longer acetylated xylooligosaccharides which migrate faster in the used solvent system. The material not treated with the enzymes contained in this fraction up to 8–10 % of total carbohydrates. GH10 xylanase converted to oligosaccharides 82% of

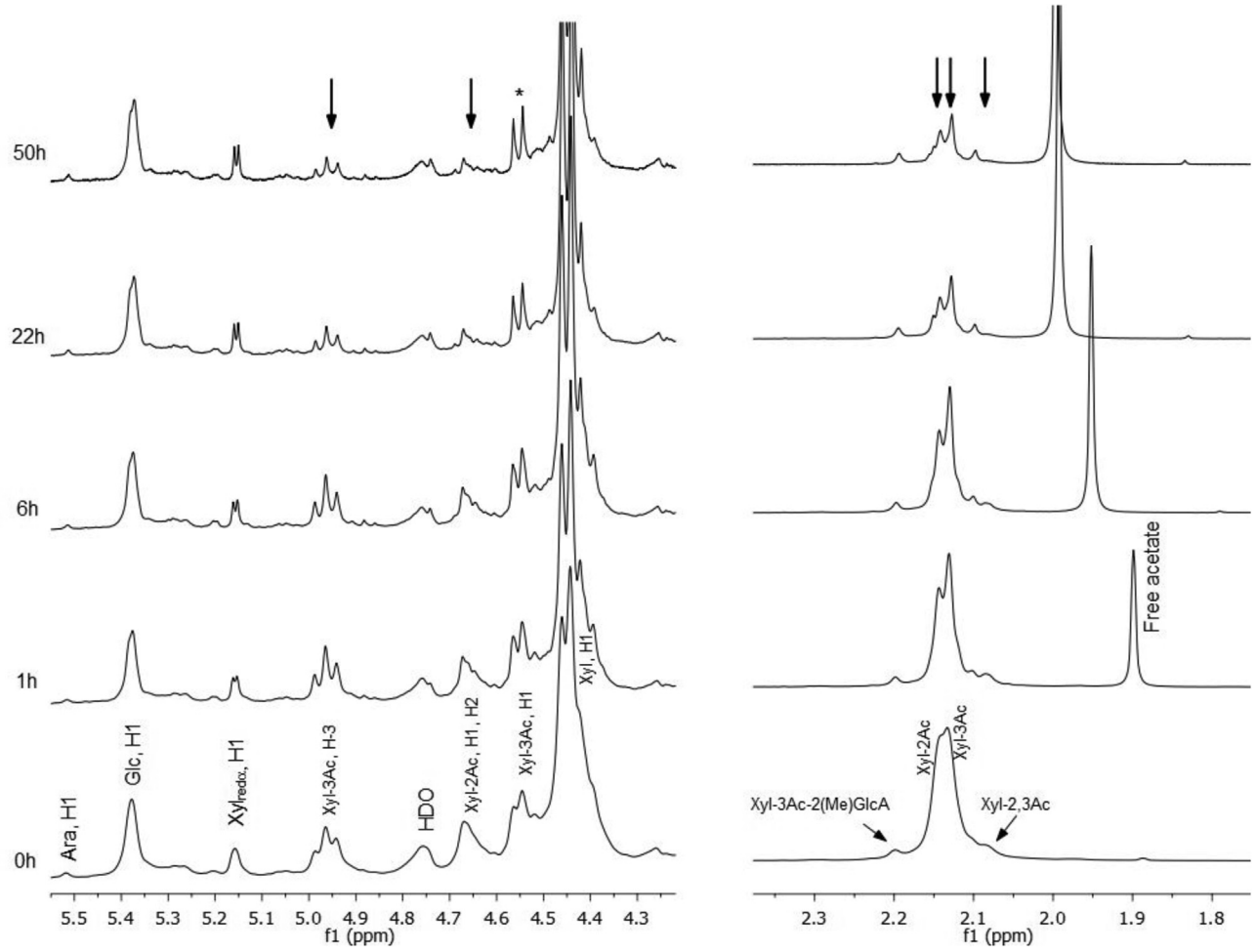

FIG. 1. Anomeric region and region of the methyl protons of the acetyl groups of the ^{1}H-NMR spectrum of CX isolated in the continuous hydrothermal reactor before (0 h) and after incubation with *Orpinomyces* CE6 AcXE (time of incubation is indicated on the left margin). Following designations of signals are used: Ara, 2-substituted Ara*f*; Glc, α-1,4-linked Glc*p*; Xyl$_{red\alpha}$, α-anomer of the reducing end Xyl; Xyl-3Ac, 3-*O*-acetylated Xyl*p*; HDO, deuterized water; Xyl-2Ac, 2-*O*-acetylated Xyl*p*; Xyl, non-acetylated Xyl*p*; Xyl-3Ac-2 (Me) GlcA, 3-*O*-acetylated Xyl*p* 2-*O*-substituted with MeGlcA; Xyl-2,3Ac, di-*O*-acetylated Xyl*p*. Asterisk marks the signal of Xyl$_{red\beta}$, H1, covered with Xyl-3Ac, H1 before deacetylation. The decreasing signals are marked by arrows.

CX, while GH11 xylanase 77%. Two-dimensional TLC of the released products in the same solvent system (Figs. S2 and S3) indicated that about one fourth of all enzyme-generated oligosaccharides was acetylated or otherwise esterified. Xyl, Xyl$_2$ and Xyl$_3$ lying on the diagonal represent the main products of both xylanases (Figs. S2 and S3).

The analysis of the enzymatic hydrolyzates of CX by xylanases belonging to GH 10 and 11 family showed that these enzymes generated considerably shorter highly acetylated and feruloylated oligosaccharides than β-xylosidase (Fig. 4C, E). This is true especially for the GH10 enzyme that acts more effectively on acetylated and branched xylan regions than GH11 (42–45). The ions of most GH10 resistant acetylated oligosaccharides contain the same or by one or two less number of acetyl groups as the number of Xyl*p* residues (e.g., Xyl$_2$Ac$_2$, Xyl$_3$Ac$_2$, Xyl$_3$Ac$_3$, Xyl$_4$Ac$_2$, Xyl$_4$Ac$_3$, Xyl$_5$Ac$_3$, Xyl$_5$Ac$_4$, and Xyl$_6$Ac$_4$). Consequently, one may envisage that CX released in the hydrothermal reactor appears to contain highly acetylated regions, resistant to the xylanases, and distributed block wise. The most remarkable effect of GH10 xylanase was the generation of significant amounts and variations of non-acetylated and acetylated AraFe-xylooligosaccharides (e.g., Xyl$_2$AraFe, Xyl$_2$AcAraFe, Xyl$_2$Ac$_2$AraFe, Xyl$_3$AraFe, Xyl$_3$AcAraFe, Xyl$_3$Ac$_2$AraFe, Xyl$_4$AraFe, Xyl$_4$AcAraFe, Xyl$_4$Ac$_2$AraFe, Xyl$_5$AraFe, Xyl$_5$AcAraFe, Xyl$_5$Ac$_2$AraFe and Xyl$_6$AraFe) (Fig. 4C). In accord with the ability of GH10 xylanases to attack the glycosidic linkages close to branches, β-xylosidase treatment of oligosaccharides generated by GH10 xylanase led to disappearance of Xyl$_2$ and Xyl$_3$ but did not alter significantly the pattern of acetylated and feruloylated oligosaccharides (Fig. 4C, D). All these products carry substituents at their non-reducing ends, but their reducing end Xyl residue remains unsubstituted (43,44).

The products of the enzymatic hydrolysis of CX by GH11 xylanase (Fig. 4E) were longer and also more diverse than those generated by GH10 xylanase (Fig. 4C), While GH10 xylanase hydrolyzed efficiently acetylated oligosaccharides larger than Xyl$_6$, oligosaccharides resistant to GH11 xylanase include those of DP 10. The shortest non-acetylated and acetylated AraFe-xylooligosaccharides are usually by one Xyl*p* residue longer than those generated by GH10 xylanase (Fig. 4C, E). The treatment of oligosaccharides generated by GH11 xylanase by β-xylosidase led to disappearance of non-acetylated xylooligosaccharides (e.g., Xyl$_4$ and Xyl$_5$ in Fig. 4E, F) but only to a modest change of the pattern of substituted oligosaccharides (Fig. 4E, F). In contrast to products of GH10 xylanase, non-reducing end Xyl*p* residue of GH11 generated oligosaccharides should not be substituted (46). The basic structural features of acetylated and branched xylooligosaccharides generated by both enzymes are shown in Fig. 5.

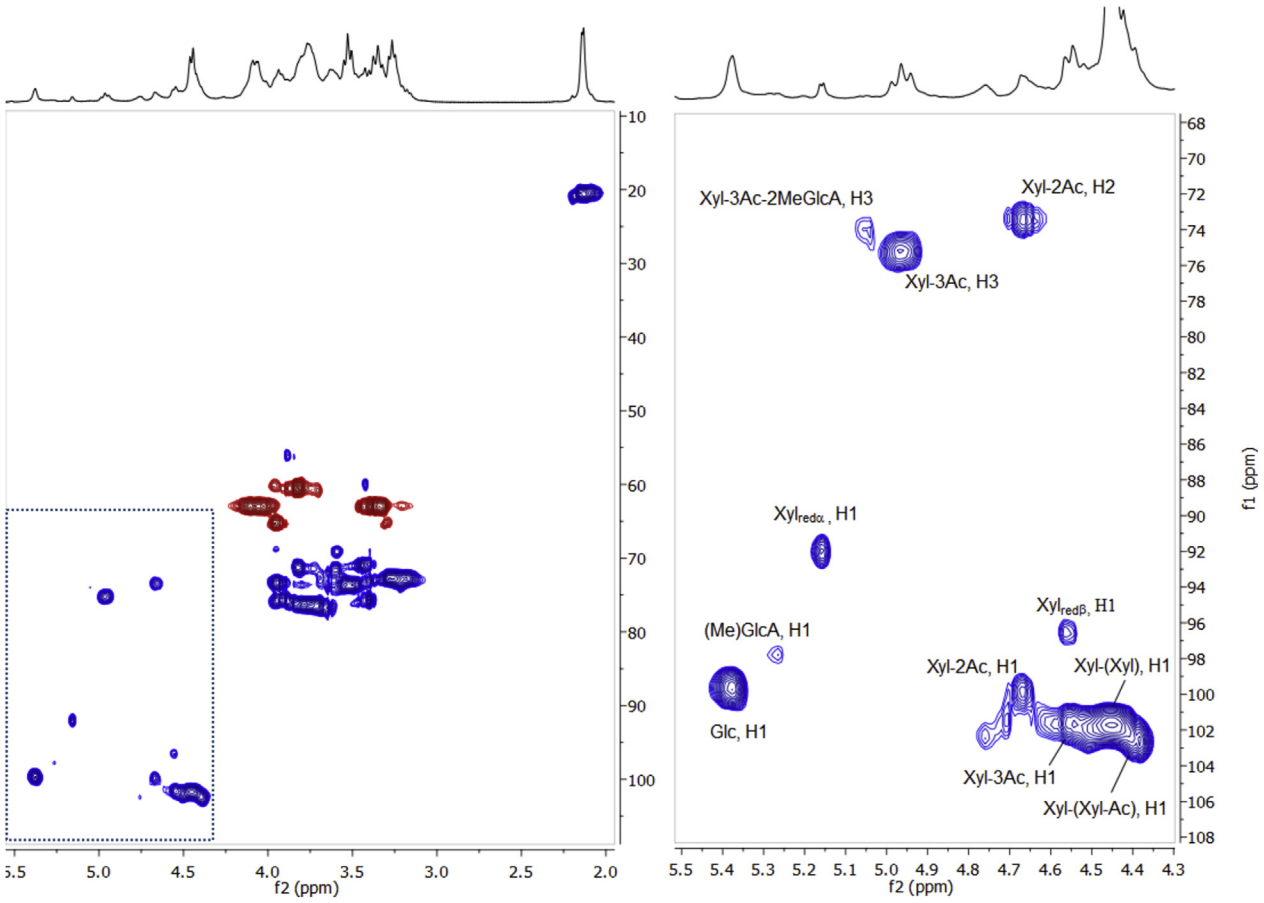

FIG. 2. The HSQC spectrum of CX (left part) and its anomeric region (the rectangle in the left part) enlarged (right part). Following designations are used: Glc, α-1,4-linked Glc*p*; Xyl$_{red\alpha}$, α-anomer of reducing end Xyl; Xyl$_{red\beta}$, β-anomer of reducing end Xyl; Xyl-3Ac, 3-*O*-acetylated Xyl*p*; Xyl-2Ac, 2-*O*-acetylated Xyl*p*; Xyl-(Xyl), non-acetylated Xyl*p*; Xyl-3Ac-2(Me)GlcA, 3-*O*-acetylated Xyl*p* 2-*O*-substituted with MeGlcA; (Me)GlcA, 4-*O*-methyl-α-D-glucuronic acid or GlcA.

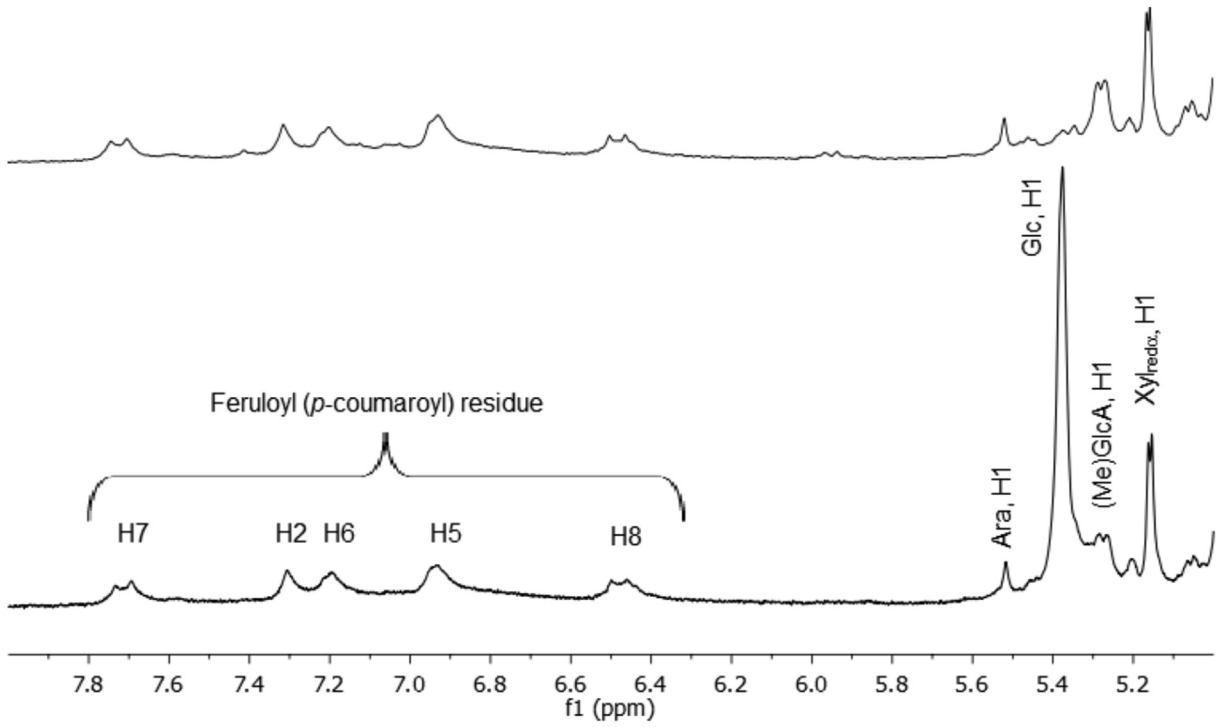

FIG. 3. Part of the ^{1}H-NMR spectrum of CX showing signals of phenolic acids and part of the anomeric region with the H1 signal of α-1,4-linked Glc*p* (bottom spectrum) which disappeared after treatment with amylolytic enzymes (spectrum on the top). The top spectrum also shows the H1 signal of MeGlcA.

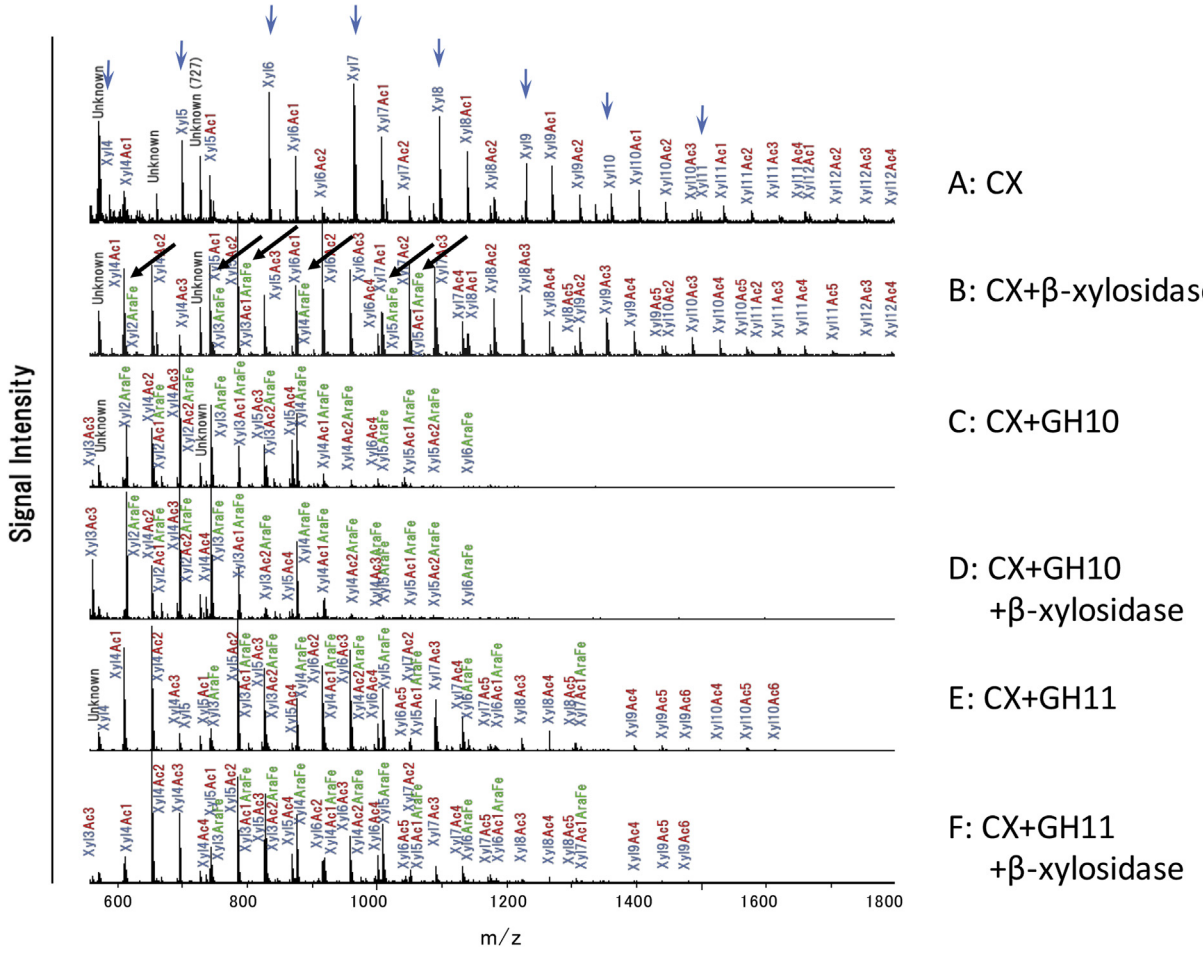

FIG. 4. MALDI-TOF MS spectra of isolated CX (A) and its enzymatic hydrolyzates by GH3 β-xylosidase (B), GH10 xylanase (C), GH10 xylanase and subsequent GH3 β-xylosidase treatment (D), GH11 xylanase (E) and GH11 xylanase and subsequent GH3 β-xylosidase treatment (F). The arrows in spectrum B point to ions of linear xylooligosaccharides that disappeared on incubation with β-xylosidase.

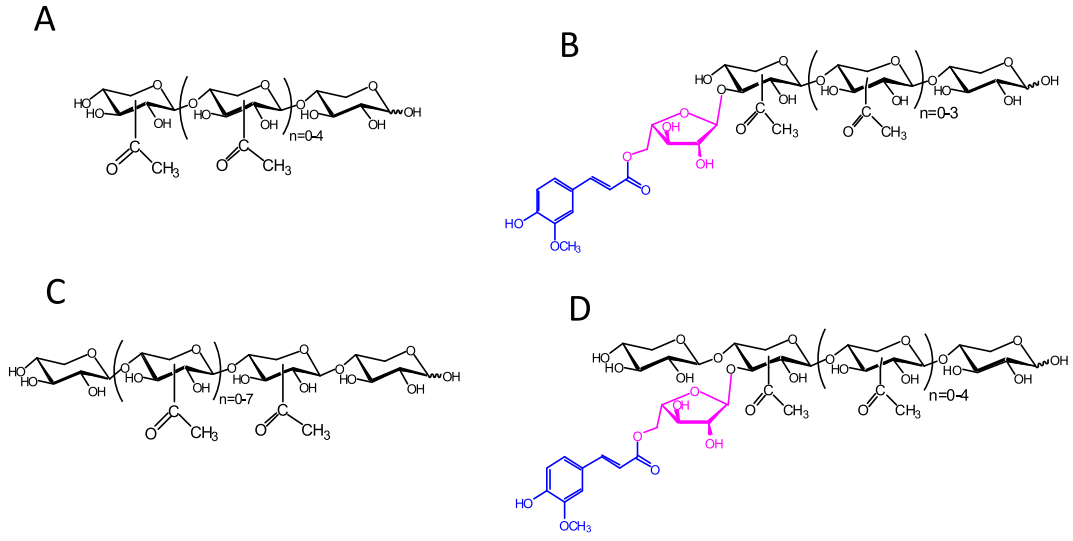

FIG. 5. Structural features of acetylated and feruloylated oligosaccharides generated from CX by GH10 (A, B) and GH11 (C, D) xylanases. The reducing-end Xyl*p* residues are unsubstituted in products of both enzymes. The non-reducing–end Xyl*p* residue could be singly or doubly substituted in products of GH10 xylanase, but should remain unsubstituted in products of GH11 xylanase. The location of the acetyl groups may vary among Xyl*p* residues and between positions 2 and 3, and some Xyl*p* residues can be non-acetylated or doubly acetylated (n rises with the overall number of acetyl groups).

Fig. 6 shows another presentation of the MALDI TOF MS analysis of isolated CX and its enzymatic hydrolyzates. We are aware that this presentation ignores all larger compounds that do not ionize under the used conditions. Fig. 6 shows that all linear xylooligosaccharides present in the starting were shortened to Xyl_2 and Xyl_3 by GH10 and GH11 xylanases, and all linear xylooligosaccharides without acetyl group completely disappeared on incubation with β-xylosidase. Acetylated oligosaccharides which were generated by GH10 xylanase, were quite resistant to β-xylosidase due to substitution on the non-reducing end. The broken lines present the groups of acetylated xylooligosaccharides based on the ratio of acetyl groups and xylose residues. In case of β-xylosidase treatment, DP of CX fraction might be decreased about three to by β-xylosidase, and DP of CX fraction with GH 11 xylanase might be about one.

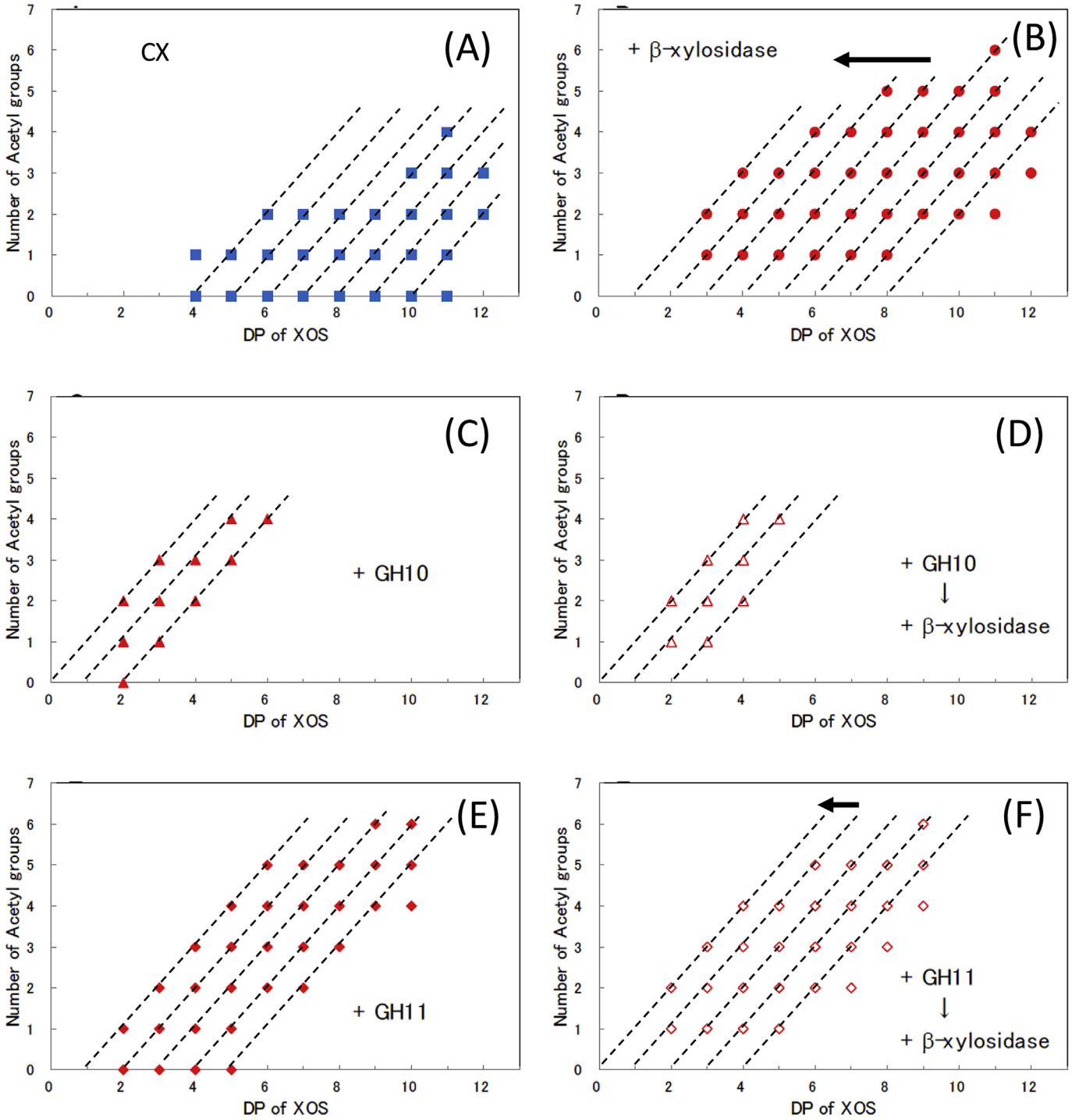

FIG. 6. Summary of MALDI TOF MS analysis of oligosaccharides of isolated CX and those formed after CX treatment with enzymes. Number of pentose residues in observed products is plotted versus the number of their acetyl groups. Oligosaccharides in the sample of isolated XOP (A); oligosaccharides after the treatment with GH3 β-xylosidase (B), GH10 xylanase (C), GH10 xylanase and subsequent treatment with GH3 β-xylosidase (following thermal denaturation of the xylanase) (D), GH11 xylanase (E) and GH11 xylanase and subsequent treatment with GH3 β-xylosidase (following thermal denaturation of the xylanase) (F).

DISCUSSION

This work extends current information on the nature of hemicellulose liberated from milled corn cob in the continual hydrothermal reactor introduced by our group (29). The hydrothermal treatment under the condition we used (190 °C, 1.8 Mpa, 13 min heating time during continuous process) leads to about 50% reduction of the content of Ara*f*. This reduction goes on account of the depletion of mainly non-esterified Ara*f*. The Xyl:Ara*f* ratio in our isolated CX was found to be much lower than in the cases of the polysaccharide extracted by hot water, mild acid or alkali (2,20,47).

A comparison of the Xyl:acetyl ratio is around 6 in isolated CX with that reported in hot water extracted corn cob polysaccharide (Xyl:acetyl is around 8) (19) indicated that the acetyl esters are quite stable during the continuous hydrothermal extraction because of acidic condition. The MALDI TOF MS analysis of oligosaccharides generated from CX by β-xylosidase, GH10 and GH11 xylanases, respectively and their combination, provided evidence that acetyl substituents are not evenly allocated on oligosaccharide chains. Formation of shorter highly acetylated and feruloylated oligosaccharides upon the action of β-xylosidase supports the view that relatively long regions of CX chains are non-substituted or scarcely acetylated. These regions give rise to short non-substituted xylooligosaccharides on incubation with xylanases leaving behind enzyme resistant highly acetylated and otherwise branched oligosaccharides. The presence of oligosaccharides like Xyl_3Ac_3, Xyl_4Ac_3 and Xyl_5Ac_4 in the xylanase hydrolyzates supports the view that less substituted parts of xylan main chain are mixed with highly acetylated regions. The observed irregularity in xylan acetylation is also interesting in view of the architecture of plant cell walls. Bromley and his colleagues (48) proposed a model of cellulose–xylan interactions determined by two differently substituted domains of the same xylan chain (molecule). The partially acetylated xylan domain, but less decorated by side chain carbohydrates, may play a role in attachment to cellulose fibrils by hydrogen bonding, while the minor, more heavily branched domain, which has a different conformation, does not interact with cellulose, but fills the space between cellulose fibrils and contributes to the three-dimensional structure of the cell wall and its hydrodynamics (49).

A similar consideration can apply to fragments with AraFe substitution, which were also singly or doubly acetylated. Why do the side residues stabilize these regions of xylan is not exactly known. One of the reasons could be the fact that both acetyl and feruloyl groups contain carbonyl groups as a primary condition for the formation of a pseudo-conjugated system. Other reason could be an agglomerate of carbohydrate and acid residues kept together by a combination of hydrogen bonding and hydrophobic interactions. A higher stability was also reported by xylan regions containing feruloylated Ara*f* side residue further branched with 2-*O*-linked Xyl*p* residue or galactosylated Xyl*p* residue (19,39,41). The sodium adduct of the fragment Pen_2Ac_2FeHex (*m*/*z* 727, marked as unknown) is visible in the spectra in Fig. 4.

The fact that the corn cob hemicellulose and its fragments released in hydrothermal reactor are partially acetylated, may be considered as advantageous in several aspects. Partial acetylation improves solubility of long xylooligosaccharides by preventing molecular interactions between the xylan and xylooligosaccharide main chains and also xylan binding to cellulose (50–52). A combination of a less severe hydrothermal reaction (27) and subsequent enzymatic reaction opens possibilities to produce various types of valuable oligosaccharides with potentially different physiological functions and applications. A population of acetylated and feruloylated products of a very narrow DP range can be generated particularly by GH10 xylanase. The esterified products can be easily separated from unsubstituted xylooligosaccharides based on different solubility or by hydrophobic interaction chromatography. Important type of esterified xylooligosaccharides are feruloylated oligosaccharides which were shown to function as dietary antioxidants (53). Moreover, feruloylated arabinoxylooligosaccharides were shown to be such a form of FeA that decreases the elimination half-life of orally administered FeA from rat blood plasma (54). Oral bioavailability of sugar-bound forms of FeA was much higher than that of free FeA (55). Linear xylooligosaccharides are known to be efficient prebiotics (26,56). Interesting that a similar potential of acetylated xylooligosacharides have not been investigated yet. The acetyl groups could have some positive effects, such as increase of the half-life of oligosaccharide in the digestive tract.

Conclusion The analysis of the structure of CX released in a continuous flow type hydrothermal reactor under the selected reaction conditions showed that its high solubility is a consequence not only of its depolymerization but also its partial acetylation and the presence of regions with relatively high degree of substitution and esterification preventing the agglomerization of xylan molecules. The isolated material can be deacetylated enzymatically by AcXE prior conversion to prebiotic xylooligosaccharides by xylanases. Without the deacetylation step CX is converted by xylanases into a mixture of non-acetylated and acetylated/ferulylated xylooligosaccharides. The presence of the acetyl and feruloyl groups could be the basis for separation of oligosaccharides into groups of compounds of different structure and different biological properties and applications. To our knowledge, prebiotic efficiency of acetylated xylooligosaccharides have not been compared with that of non-acetylated counterparts. To isolate CX with maximum possible degree of acetylation in our continuous hydrothermal reactor could be a new challenge. Severity of the extraction conditions has been shown to affect the xylan acetylation in a batch hydrothermal reactor (27). Currently we are working on scale up of the described extraction procedure and application of the continuous hydrothermal reactor to other plant materials.

Supplementary data related to this article can be found at https://doi.org/10.1016/j.jbiosc.2018.07.016.

ACKNOWLEDGMENTS

Technical assistance of Mrs. Mária Cziszárová is greatly appreciated. Our thanks are due to Dr. Vladimír Puchart for several MALDI TOF MS measurements and helpful discussions. This study was performed under the Development of Technology for High Efficiency Bioenergy Conversion Project supported by New Energy and Industrial Technology Development Organization (NEDO), Japan.

References

1. **Gírio, F. M., Fonseca, C., Carvalheiro, F., Duarte, L. C., Marques, S., and Bogel-Łukasik, R.:** Hemicelluloses for fuel ethanol: a review, Bioresour. Technol., **101**, 4775–4800 (2010).
2. **Van Dongen, F. E. M., Van Eylen, D., and Kabel, M. A.:** Characterization of substituents in xylans from corn cobs and stover, Carbohydr. Polym., **86**, 722–731 (2011).
3. **Rennie, E. A. and Scheller, H. V.:** Xylan biosynthesis, Curr. Opin. Biotechnol., **26**, 100–107 (2014).
4. **Teleman, A., Lundqvist, J., Tjerneld, F., Stålbrand, H., and Dahlman, O.:** Characterization of acetylated 4-*O*-methylglucuronoxylan isolated from aspen employing ^1H and ^{13}C NMR spectroscopy, Carbohydr. Res., **329**, 807–815 (2000).
5. **Teleman, A., Tenkanen, M., Jacobs, A., and Dahlman, O.:** Characterization of *O*-acetyl-(4-*O*-methylglucurono) xylan isolated from birch and beech, Carbohydr. Res., **337**, 373–377 (2002).
6. **Naran, R., Black, S., Decker, S. R., and Azadi, P.:** Extraction and characterization of native heteroxylans from delignified corn stover and aspen, Cellulose, **16**, 661–675 (2009).
7. **Pawar, P. M.-A., Koutaniemi, S., Tenkanen, M., and Mellerowicz, E. J.:** Acetylation of woody lignocellulose: significance and regulation, Front. Plant Sci., **4**, 118 (2013).

8. **Pauly, M., Gille, S., Liu, L., Mansoori, N., de Souza, A., Schultink, A., and Xiong, G.:** Hemicellulose biosynthesis, Planta, **238**, 627–642 (2013).
9. **Williamson, G., Kroon, P. A., and Faulds, C. B.:** Hairy plant polysaccharides: a close shave with microbial esterases, Microbiology, **144**, 2011–2023 (1998).
10. **Deutschmann, R. and Dekker, R. F. H.:** From plant biomass to bio-based chemicals: latest developments in xylan research, Biotechnol. Adv., **30**, 1627–1640 (2012).
11. **Peng, F., Peng, P., Xu, F., and Sun, R.-C.:** Fractional purification and bioconversion of hemicelluloses, Biotechnol. Adv., **30**, 879–903 (2012).
12. **Biely, P.:** Microbial carbohydrate esterases deacetylating plant polysaccharides, Biotechnol. Adv., **30**, 1575–1588 (2012).
13. **Alvira, P., Tomás-Pejó, E., Ballesteros, M., and Negro, M. J.:** Pretreatment technologies for an efficient bioethanol production process based on enzymatic hydrolysis, Bioresour. Technol., **101**, 4951–4961 (2010).
14. **Yang, B. and Wyman, C. E.:** Pretreatment: the key to unlocking low-cost cellulosic ethanol, Biofuel. Bioprod. Biorefin., **2**, 26–40 (2008).
15. **Hendriks, A. T. W. M. and Zeeman, G.:** Pretreatments to enhance the digestibility of lignocellulosic biomass, Bioresour. Technol., **100**, 10–18 (2009).
16. **Kumar, P., Barrett, D. M., Delwiche, M. J., and Stroeve, P.:** Methods for pretreatment of lignocellulosic biomass for efficient hydrolysis and biofuel production, Ind. Eng. Chem. Res., **48**, 3713–3729 (2009).
17. **Garrote, G., Dominquez, H., and Parajo, J. C.:** Mild autohydrolysis: an environmentally friendly technology for xylooligosaccharide production from wood, J. Chem. Technol. Biotechnol., **74**, 1101–1109 (1999).
18. **Vazquez, M. J., Alonso, J. L., Dominguez, H., and Parajo, J. C.:** Xylooligosaccharides: manufacture and applications, Trends Food Sci. Technol., **11**, 387–393 (2000).
19. **Kabel, M. A., Carvalheiro, F., Garrote, G., Avgerinos, E., Koukios, E., Parajó, J. C., Gírio, F. M., Schols, H. A., and Voragen, A. G. J.:** Hydrothermally treated xylan rich by-products yield different classes of xylo-oligosaccharides, Carbohydr. Polym., **50**, 47–56 (2002).
20. **Kabel, M. A., Schols, H. A., and Voragen, A. G. J.:** Complex xylo-oligosaccharides identified from hydrothermally treated *Eucalyptus* wood and brewery's spent grain, Carbohydr. Polym., **50**, 191–200 (2002).
21. **Kabel, M. A., de Waard, P., Schols, H. A., and Voragen, A. G. J.:** Location of *O*-acetyl substituents in xylo-oligosaccharides obtained from hydrothermally treated *Eucalyptus* wood, Carbohydr. Res., **338**, 69–77 (2003).
22. **Parajo, J. C., Garrote, G., Cruz, J. M., and Dominguez, H.:** Production of xylooligosaccharides by autohydrolysis of lignocellulosic materials, Trends Food Sci. Technol., **15**, 115–120 (2004).
23. **Wayman, C. E., Dale, B. E., Elander, R. T., Holzapple, M., Ladish, M. R., and Lee, Y. Y.:** Coordinated development of leading biomass pretreatment technologies, Bioresour. Technol., **96**, 1959–1966 (2005).
24. **Vazquez, M. J., Alonso, J. L., Dominguez, H., and Parajo, J. C.:** Enhancing the potential of oligosaccharides from corn cob autohydrolysis as prebiotic food ingredients, Ind. Crop. Prod., **24**, 152–159 (2006).
25. **Mood, S. H., Golfeshan, A. H., Tabatabaei, M., Jouzani, G. S., Najafi, G. H., Gholami, M., and Ardjmand, M.:** Lignocellulosic biomass to bioethanol, a comprehensive review with a focus on pretreatment, Renew. Sustain. Energy Rev., **27**, 77–93 (2013).
26. **Qing, Q., Li, H., Kumar, R., and Wyman, C. E.:** Aqueous xylooligosaccharides production, quantification, and characterization in context of lignocellulosic, pp. 391–415, in: Wyman, C. E. (Ed.), Pretreatment of plant biomass for biological and chemical conversion to fuels and chemicals, 1st ed. John Wiley & Sons, Ltd. (2013).
27. **Garrote, G., Dominquez, H., and Parajo, J. C.:** Interpretation of deacetylation and hemicellulose hydrolysis during hydrothermal treatments on the basis of the severity factor, Process Biochem., **37**, 1067–1073 (2002).
28. **Garrote, G., Dominquez, H., and Parajo, J. C.:** Autohydrolysis of corn cob: study of non-isothermal operation for xylooligosaccharide production, J. Food Eng., **52**, 211–218 (2002).
29. **Makishima, S., Mizuno, M., Sato, N., Shinji, K., Suzuki, M., Nozaki, K., Takahashi, F., Kanda, T., and Amano, Y.:** Development of continuous flow type hydrothermal reactor for hemicellulose fraction recovery from corn cob, Bioresour. Technol., **100**, 2842–2848 (2009).
30. **Sato, N., Shinji, K., Mizuno, M., Nozaki, K., Suzuki, M., Makishima, S., Shiroishi, M., Onoda, T., Takahashi, F., Kanda, T., and Amano, Y.:** Improvement in the productivity of xylooligosaccharides from waste medium after mushroom cultivation by hydrothermal treatment with suitable pretreatment, Bioresour. Technol., **101**, 6006–6011 (2010).
31. **Sato, N., Takano, Y., Mizuno, M., Nozaki, K., Umemura, S., Matsuzawa, T., Amano, Y., and Makishima, S.:** Production of feruloylated arabino-oligosaccharides (FA-AOs) from beet fiber by hydrothermal treatment, J. Supercrit. Fluids, **79**, 84–91 (2013).
32. **Blumenkrantz, N. and Asboe-Hansen, G.:** New method for quantitative determination of uron ic acids, Anal. Biochem., **54**, 484–489 (1973).
33. **Kuno, A., Shimizu, D., Kaneko, S., Koyama, Y., Kobayashi, H., Hayashi, K., Taira, K., and Kusakabe, I.:** PCR cloning and expression of the F/10 family xylanase gene from *Streptomyces olivaceoviridis* E-86, J. Ferment. Bioeng., **86**, 434–439 (1998).
34. **Kaneko, S., Kuno, A., Muramatsu, M., Iwamatsu, S., Kusakabe, I., and Hayashi, K.:** Purification and characterization of a family G/11 β-xylanase from *Streptomyces olivaceoviridis* E-86, Biosci. Biotechnol. Biochem., **64**, 447–451 (2000).
35. **Uhliariková, I., Vršanská, M., McCleary, B. V., and Biely, P.:** Positional specifity of acetylxylan esterases on natural polysaccharide: an NMR study, Biochim. Biophys. Acta, **1830**, 3365–3372 (2013).
36. **Christov, L., Biely, P., Kalogeris, E., Christakopoulos, P., Prior, B. A., and Bhat, M. K.:** Effects of purified endo-β-1,4-xylanases of family 10 and 11 and acetyl xylan esterases on eucalypt sulfite dissolving pulp, J. Biotechnol., **83**, 231–244 (2000).
37. **Bounias, M.:** *N*-(1-Naphthyl)ethylenediamine dihydrochloride as a new reagentfor nanomole quantification of sugars on thin-layer plates by a mathematical calibration process, Anal. Biochem., **106**, 291–295 (1980).
38. **Appeldoorn, M. M., de Ward, P., Kabel, M. A., Gruppen, H., and Schols, H. A.:** Enzyme resistant ferulated xylooligomer analogues from thermochemically treated corn fiber containlarge side chains, ethyl glycosides and novel sites of acetylation, Carbohydr. Res., **381**, 33–42 (2013).
39. **Dubois, M. K., Gilles, A., Hamilton, J. K., Rebers, P. A., and Smith, F.:** Colorimetric method for determination of sugars and related substances, Anal. Chem., **28**, 350–356 (1956).
40. **Schendel, R. R., Becker, A., Tyl, C. E., and Bunzel, M.:** Isolation and characterization of feruloylated arabinoxylan oligosaccharides from the perennial cereal grain intermediate wheat grass (*Thinopyrum intermedium*), Carbohydr. Res., **407**, 16–25 (2015).
41. **Ebringerová, A. and Heinze, T.:** Xylan and xylan derivatives – biopolymers with valuable properties, 1. Naturally occurring xylanas structures, isolation procedures and properties, Macromolecul. Rapid. Commun., **21**, 542–556 (2000).
42. **Biely, P., Vršanská, M., Tenkanen, M., and Kluepfel, D.:** Endo-β-1,4-xylanase families: differences in catalytic properties, J. Biotechnol., **57**, 151–166 (1997).
43. **Pell, G., Taylor, E. J., Gloster, T. M., Turkenburg, J. P., Fontes, C. M. G. A., Ferreira, L. M. A., Nagy, T., Clark, S. J., Davies, G. J., and Gilbert, H. J.:** The mechanism by which family 10 glycoside hydrolases bind decorated substrates, J. Biol. Chem., **279**, 9597–9605 (2004).
44. **Fujimoto, Y., Kaneko, S., Kuno, A., Kobayashi, H., Kusakabe, I., and Mizuni, H.:** Crystal structures of decorated xylooligosaccharides bound to family 10 xylanase from *Streptomyces olivoceoviridis*, J. Biol. Chem., **279**, 9606–9614 (2004).
45. **Kolenová, K., Vrsanská, M., and Biely, P.:** Mode of action of endo-β-1,4-xylanases of families 10 and 11 on acidic xylooligosaccharides, J. Biotechnol., **121**, 338–345 (2006).
46. **Wan, Q., Zhang, Q., Hamilton-Brehm, S., Weiss, K., Mustyakimov, M., Coates, L., Langan, P., Graham, D., and Kovalevsky, A.:** X-ray crystallographic studies of family 11 xylanase Michaelis and product complexes: implications for the catalytic mechanism, Acta Crystallogr. D Biol. Crystallogr., **70**, 11–23 (2014).
47. **Pellerin, P., Gosselin, M., Lepoutre, J.-P., Samain, E., and Debeire, P.:** Enzymic production of oligosaccharides from corn cob xylan, Enzyme Microb. Technol., **13**, 617–621 (1991).
48. **Bromley, J. R., Busse Wicher, M., Tryfona, T., Mortimer, J. C., Zhang, Z., Brown, D. M., and Dupree, P.:** GUX1 and GUX2 glucuronyltransferases decorate distinct domains of glucuronoxylan with different substitution patterns, Plant J., **74**, 423–434 (2013).
49. **Busse-Wicher, M., Gomes, T. C. F., Tryfona, T., Nikolovski, N., Stott, K., Grantham, N. J., Bolam, D. N., Skaf, M. S., and Dupree, P.:** The pattern of xylan acetylation suggests xylan may interact with cellulose microfibrils as a twofold helical screw in the secondary plant cell wall of *Arabidopsis thaliana*, Plant J., **79**, 492–506 (2014).
50. **Biely, P., MacKenzie, C. R., and Schneider, H.:** Production of acetylxylan esterase by *Trichoderma reesei* and *Schizophyllum commune*, Can. J. Microbiol., **34**, 767–772 (1988).
51. **Köhnke, T., Ostlund, A., and Brelid, H.:** Adsorption of arabinoxylan on cellulosic surfaces: influence of degree of substitution and substitution pattern on adsorption characteristics, Biomacromolecules, **12**, 2633–2641 (2011).
52. **Bosmans, T. J., Stépán, A. M., Toriz, G., Renneckar, S., Karabulut, E., Wågberg, L., and Gatenholm, P.:** Assembly of debranched xylan from solution and on nanocellulosic surfaces, Biomacromolecules, **15**, 924–930 (2014).
53. **Katapodis, P., Vardakou, M., Kalogeris, E., Kekos, D., Macris, B. J., and Christakopoulos, P.:** Enzymic production of a feruloylated oligosaccharide with antioxidant activity from wheat flour arabinoxylan, Eur. J. Nutr., **42**, 55–60 (2003).
54. **Zhao, Z., Egashira, Y., and Sanada, H.:** Ferulic acid sugar esters are recovered in rat plasma and urine mainly as the sulfoglucuronide of ferulic acid, J. Nutr., **133**, 1355–1361 (2003).
55. **Rondini, L., Peyrat-Maillard, M.-N., Marsset-Baglieri, A., Fromentin, G., Durand, P., Tomé, D., Prost, M., and Berset, C.:** Bound ferulic acid from bran is more bioavailable than the free compound in rat, J. Agric. Food Chem., **52**, 4338–4343 (2004).
56. **Broekaert, W. F., Courtin, C. M., Verbeke, K., Van de Wiele, T., Verstraete, W., and Delcour, J. A.:** Prebiotic and other health-related effects of cereal-derived arabinoxylans, arabinoxylan-oligosaccharides, and xylooligosaccharides, Crit. Rev. Food Sci. Nutr., **51**, 178–194 (2011).